INFLUENCE OF THERMOPHORESIS AND JOULE HEATING ON THE RADIATIVE FLOW OF JEFFREY FLUID WITH MIXED CONVECTION

S. A. Shehzad[1*], A. Alsaedi[2] and T. Hayat[1,2]

[1]Department of Mathematics, Quaid-i-Azam University 45320,
Islamabad 44000, Pakistan.
[2]Department of Mathematics, Faculty of Science, King Abdulaziz University,
P.O. Box 80257, Jeddah 21589, Saudi Arabia.
E-mail: ali_qau70@yahoo.com

Abstract - The aim of the present study is to address the magnetohydrodynamic (MHD) radiative flow of an incompressible Jeffrey fluid over a linearly stretched surface. Heat and mass transfer characteristics are accounted for in the presence of Joule heating and thermophoretic effects. Series solutions by the homotopy analysis method are constructed for the velocity, temperature and concentration fields. A convergence criterion for the series solutions is discussed. In addition, the numerical values of the skin friction coefficient, local Nusselt and Sherwood numbers are first computed and then analyzed.
Keywords: Radiative flow; MHD Jeffrey fluid; Joule heating; Thermophoresis.

INTRODUCTION

The analysis of non-Newtonian fluids is significant because of several industrial and engineering applications. Such fluids are encountered in the process of manufacturing coated sheets, foods, drilling muds, cosmetic products, dilute polymer solutions, polymeric melts etc. Different models of such fluids have beenare suggested. This is due to the versatility of fluid characteristics in nature (Qi and Xu, 2007; Kothandapani and Srinivas, 2008; Nadeem and Akbar, 2010; Jamil and Fetecau, 2010a,b; Wang and Tan, 2011; Hayat et al., 2011a,b; Jamil et al., 2011; Nadeem et al., 2011; Hayat et al., 2012). Although much information is available on the boundary layer flow of viscous fluids, such attempts for non-Newtonian fluids are limited. In fact, the resulting differential equations in non-Newtonian fluids are more nonlinear than for a viscous fluid. To find the analytic/numerical solution of such equations is not an easy task.

Investigation of heat transfer in the boundary layer over a stretching sheet has key importance in extrusion processes, paper production, glass drawing, electronic chips, crystal growing, plastic manufacture, metal spinning and cooling of metallic plates in a cooling bath etc. For the quality of the final product in such processes, the cooling rate has great relevance (Bhattacharyya et al., 2001; Hayat et al., 2010; Rashidi and Pour, 2010; Vyas and Rai, 2010; Yao et al., 2011; Rashidi and Erfani, 2011; Rashidi et al., 2011; Makinde and Aziz, 2011; Sahoo and Poncet, 2011). The migration of small particles in the direction of decreasing thermal gradient is called thermophoresis (Hinds, 1982). This is used for particle collection. The velocity gained by the particle is called the thermophoretic velocity and the force experienced by the suspended particle due to the temperature difference is called the thermophoretic force (Tasai et al., 2004). Thermophoresis is a mechanism for particles on a cold surface. It is quite significant in aerosol particle sampling, deposition of

silicon thin films, radioactive particle deposition in nuclear reactor safety simulations, scale formation on surfaces of heat exchangers, microelectronic manufacturing, particulate material deposition on turbine blades, modified chemical vapour deposition etc. Goren (1977) studied the laminar flow of a viscous fluid with thermophoresis in the presence of cold and hot plate conditions. The effect of thermophoresis in MHD flow of a viscous fluid over an inclined plate was anlyzed by Aslam *et al.* (2008). Hayat and Qasim (2010) investigated the radiative flow of Maxwell fluid in the presence of Joule heating and thermophoresis effects. Hayat and Alsaedi (2011) further examined the thermophoresis effects in MHD flow of Oldroyd-B fluid over a linearly stretching surface. Heat and mass transfer effects in the thermophoretic flow of viscous fluid over an inclined isothermal permeable surface have been explored by Noor *et al.* (2012).

Motivated by the above mentioned studies, the aim here is to investigate the effects of thermophoresis in MHD flow of a non-Newtonian fluid over a stretching surface. Mathematical modelling is presented using constitutive equations of a Jeffrey fluid. Thermal radiation and Joule heating effects are taken into account. The present study is structured in the following fashion. The mathematical formulation is completed in the next section. Series solutions by the homotopy analysis method (HAM) (Liao, 2003; Yao, 2009; Rashidi *et al.*, 2011b; Hayat *et al.*, 2011c; Vosughi *et al.*, 2011; Aziz *et al.*, 2012; Hayat *et al.*, 2011d) are developed in the subsequent sections. Then convergence analysis and discussion are presented. Important results are summarized in the last section.

FLOW FORMULATION

We consider Cartesian coordinate system in such a way that the $x-$axis is along the stretching surface and the $y-$axis is perpendicular to the $x-$axis. Magnetohydrodynamic boundary layer flow of a Jeffrey fluid is considered. A uniform magnetic field $\mathbf{B}_0$ is applied parallel to the $y-$axis (see Figure 1). The induced magnetic field is neglected for small magnetic Reynolds number. Heat and mass transfer characteristics are taken into account in the presence of thermal radiation and thermophoresis effects. The uniform temperature of the surface T_w is larger than the ambient fluid temperature T_∞.
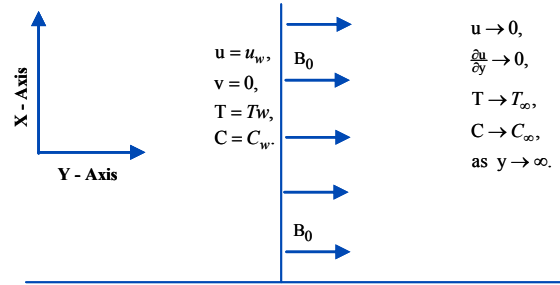
Figure 1: Physical model

The species concentration at the surface C_w and ambient concentration C_∞ are constants. Invoking the Rosseland approximation [24], the resulting equations take the following forms:

$$\frac{\partial u}{\partial x} + \frac{\partial v}{\partial y} = 0, \tag{1}$$

$$u\frac{\partial u}{\partial x} + v\frac{\partial u}{\partial y} = \frac{\nu}{1+\lambda_1}\left(\frac{\partial^2 u}{\partial y^2} + \lambda_2\left(\begin{array}{c} u\dfrac{\partial^3 u}{\partial x \partial y^2} + v\dfrac{\partial^3 u}{\partial y^3} \\ -\dfrac{\partial u}{\partial x}\dfrac{\partial^2 u}{\partial y^2} + \dfrac{\partial u}{\partial y}\dfrac{\partial^2 u}{\partial x \partial y} \end{array}\right)\right)$$
$$-\frac{\sigma^* B_0^2}{\rho}u + g[\beta_T(T-T_\infty) + \beta_c(C-C_\infty)], \tag{2}$$

$$u\frac{\partial T}{\partial x} + v\frac{\partial T}{\partial y} = \frac{k}{\rho c_p}\frac{\partial^2 T}{\partial y^2} + \frac{16\sigma T_\infty^3}{3k^*}\frac{\partial^2 T}{\partial y^2}$$
$$+ \frac{\mu}{\rho c_p}\left(\frac{\partial u}{\partial y}\right)^2 + \frac{\sigma^* B_0^2}{\rho c_p}u^2, \tag{3}$$

$$u\frac{\partial C}{\partial x} + v\frac{\partial C}{\partial y} = D\frac{\partial^2 C}{\partial y^2} - \frac{\partial}{\partial y}(V_T C). \tag{4}$$

Here (u,v) are the velocity components along the $x-$ and $y-$axes, λ_1 and λ_2 are the ratio of relaxation/retardation times and retardation time, respectively, ν the dynamic viscosity, ρ the density of the fluid, σ^* the electrical conductivity, g the gravitational acceleration, β_T and β_c the thermal expansion coefficients, T the temperature, c_p the specific heat, σ the Stefan-Boltzmann constant, k^* the mean absorption coefficient, D the diffusion coefficient and V_T the thermophoretic velocity.

The associated boundary conditions are:

$$u = u_w = ax, \; v = 0, \; T = T_w(x), \; C = C_w(x)$$

at $y = 0$,

$$u \to 0, \; \frac{\partial u}{\partial y} \to 0, \; T \to T_\infty, \; C \to C_\infty \qquad (5)$$

as $y \to \infty$.

where u_w is the stretching velocity, T_w is the temperature at the wall, C_w is the concentration at the wall and T_∞ and C_∞ are the ambient fluid temperature and concentration, respectively.

The term V_T in Eq. (4) can be defined as follows:

$$V_T = -k_1 \frac{\nu}{T_r} \frac{\partial T}{\partial y}, \qquad (6)$$

in which k_1 is the thermophoretic coefficient and T_r is the reference temperature. A thermophoretic parameter τ is defined by the following relation:

$$\tau = -\frac{k_1(T_w - T_\infty)}{T_r}. \qquad (7)$$

The wall temperature and concentration fields are:

$$T_w = T_\infty + bx, \; C_w = C_\infty + cx, \qquad (8)$$

where a, b and c are the positive constants.

Through the following transformations:

$$u = axf'(\eta), \; v = -\sqrt{a\nu}\, f(\eta), \; \eta = y\sqrt{\frac{a}{\nu}}$$

$$\theta(\eta) = \frac{T - T_\infty}{T_w - T_\infty}, \; \phi(\eta) = \frac{C - C_\infty}{C_w - C_\infty} \qquad (9)$$

Equation (1) is automatically satisfied and Eqs. (2)-(4) are reduced as follows:

$$f''' + (1+\lambda_1)(ff'' - f'^2) + \beta(f''^2 - ff'''')$$
$$- (1+\lambda_1)Mf' + (1+\lambda_1)\gamma(\theta + N\phi) = 0, \qquad (10)$$

$$(1 + \frac{4}{3}R)\theta'' + \Pr[f\theta' - \theta f'] + \Pr Ec f''^2$$
$$+ M \Pr Ec f'^2 = 0, \qquad (11)$$

$$\phi'' + Sc(f\phi' - \phi f') - Sc\tau(\phi'\theta' - \phi\theta'') = 0, \qquad (12)$$

$$f = 0, \; f' = 1, \; \theta = 1, \; \phi = 1 \text{ at } \eta = 0,$$

$$f' \to 0, f'' \to 0, \; \theta \to 0, \; \phi \to 0 \text{ as } \eta \to \infty. \qquad (13)$$

In the above expressions, $\beta = \lambda_2 a$ is the Deborah number, $M = \sigma^* B_0^2 / \rho c$ the Hartmann number, $\gamma = \dfrac{Gr_x}{Re_x^2}$ the local buoyancy parameter, $Gr_x = \dfrac{g\beta_T(T_w - T_\infty)x^3/\nu^2}{u_w^2 x^2 / \nu^2}$ the local Grashof number, $N = \dfrac{\beta_c(C_w - C_\infty)}{\beta_T(T_w - T_\infty)}$ the constant dimensionless concentration buoyancy parameter, $\Pr = \dfrac{\mu c_p}{k}$ the Prandtl number, $R = \dfrac{4\sigma^* T_\infty^3}{k^* k}$ the radiation parameter, $Ec = \dfrac{u_w^2}{c_p(T_w - T_\infty)}$ the Eckert number and $Sc = \dfrac{\nu}{D}$ the Schmidt number.

The skin friction coefficient, local Nusselt number and local Sherwood number are transformed to the following:

$$Re_x^{1/2} C_f = \frac{1}{1+\lambda_1}\left(f''(0) + \beta f''(0)\right), Nu_x Re_x^{-1/2}$$
$$= -\theta'(0), \text{ and } Sh\, Re_x^{-1/2} = -\phi'(0). \qquad (14)$$

SERIES SOLUTIONS

The homotopic solutions for f, θ and ϕ in a set of base functions:

$$\{\eta^k \exp(-n\eta), \; k \geq 0, n \geq 0\} \qquad (15)$$

can be written to the following expressions:

$$f_m(\eta) = \sum_{n=0}^{\infty}\sum_{k=0}^{\infty} a_{m,n}^k \eta^k \exp(-n\eta), \qquad (16)$$

$$\theta_m(\eta) = \sum_{n=0}^{\infty}\sum_{k=0}^{\infty} b_{m,n}^k \eta^k \exp(-n\eta), \qquad (17)$$

$$\phi_m(\eta) = \sum_{n=0}^{\infty}\sum_{k=0}^{\infty} c_{m,n}^k \eta^k \exp(-n\eta), \qquad (18)$$

in which $a_{m,n}^k$, $b_{m,n}^k$ and $c_{m,n}^k$ are the coefficients. Initial guesses and the auxiliary linear operators are

$$f_0(\eta) = (1-\exp(-\eta),\ \theta_0(\eta)$$
$$= \exp(-\eta),\ \phi_0(\eta) = \exp(-\eta), \qquad (19)$$

$$L_f = f''' - f',\ L_\theta = f'' - f,\ L_\phi = f'' - f. \qquad (20)$$

The operators in Eq. (19) satisfy the following properties:

$$L_f(C_1 + C_2 e^{\eta} + C_3 e^{-\eta}) = 0,\ L_\theta(C_4 e^{\eta} + C_5 e^{-\eta})$$
$$= 0,\ L_\phi(C_6 e^{\eta} + C_7 e^{-\eta}), \qquad (21)$$

where $C_i\ (i = 1-7)$ denote the arbitrary constants. The zeroth order deformation problems are expressible in the form

$$(1-q)L_f\left(\hat{f}(\eta;q) - f_0(\eta)\right) =$$
$$q\hbar_f \mathbf{N}_f\left(\hat{f}(\eta;q), \hat{\theta}(\eta;q), \hat{\phi}(\eta;q)\right), \qquad (22)$$

$$(1-q)L_\theta\left(\hat{\theta}(\eta;q) - \theta_0(\eta)\right) =$$
$$q\hbar_\theta \mathbf{N}_\theta\left(\hat{\theta}(\eta;q), \hat{f}(\eta;q), \hat{\phi}(\eta;q)\right), \qquad (23)$$

$$(1-q)L_\phi\left(\hat{\phi}(\eta;q) - \phi_0(\eta)\right) =$$
$$q\hbar_\phi \mathbf{N}_\phi\left(\hat{\theta}(\eta;q), \hat{f}(\eta;q), \hat{\phi}(\eta;q)\right), \qquad (24)$$

$$\hat{f}(0;q) = 0,\ \hat{f}'(0;q) = 1,\ \hat{f}'(\infty;q) = 0,\ \hat{f}''(\infty;q) = 0,$$
$$\hat{\theta}(0;q) = 1,\ \hat{\theta}(\infty;q) = 0,\ \hat{\phi}(0;q) = 1\ \text{and}\ \hat{\phi}(\infty;q) = 0. \qquad (25)$$

Here q is the embedding parameter, $\hbar_f$, $\hbar_\theta$ and $\hbar_\phi$ the non-zero auxiliary parameters and the nonlinear operators $\mathbf{N}_f$, $\mathbf{N}_\theta$ and $\mathbf{N}_\phi$ are given by:

$$\mathbf{N}_f[\hat{f}(\eta,q), \hat{\theta}(\eta;q), \hat{\phi}(\eta;q)] = \frac{\partial^3 \hat{f}(\eta,q)}{\partial\eta^3} + (1+\lambda_1)\left(\hat{f}(\eta,q)\frac{\partial^2 \hat{f}(\eta,q)}{\partial\eta^2} - \left(\frac{\partial\hat{f}(\eta,q)}{\partial\eta}\right)^2\right)$$
$$+\beta\left(\left(\frac{\partial^2 \hat{f}(\eta,q)}{\partial\eta^2}\right)^2 - \hat{f}(\eta,q)\frac{\partial^4 \hat{f}(\eta,q)}{\partial\eta^4}\right) - (1+\lambda_1)M\frac{\partial\hat{f}(\eta,q)}{\partial\eta} \qquad (26)$$
$$+(1+\lambda_1)\left(\gamma(\hat{\theta}(\eta,q) + N\hat{\phi}(\eta;q)\right),$$

$$\mathbf{N}_\theta[\hat{f}(\eta,q), \hat{\theta}(\eta;q), \hat{\phi}(\eta;q)] = \left(1+\frac{4}{3}R\right)\frac{\partial^2\hat{\theta}(\eta,q)}{\partial\eta^2} + \Pr Ec\left(\frac{\partial^2 \hat{f}(\eta,q)}{\partial\eta^2}\right)^2 + M\Pr Ec\left(\frac{\partial\hat{f}(\eta,q)}{\partial\eta}\right)^2$$
$$-\Pr\hat{\theta}(\eta,q)\frac{\partial\hat{f}(\eta,q)}{\partial\eta} + \Pr\hat{f}(\eta,q)\frac{\partial\hat{\theta}(\eta,q)}{\partial\eta}, \qquad (27)$$

$$\mathbf{N}_\phi[\hat{f}(\eta,q), \hat{\theta}(\eta;q), \hat{\phi}(\eta;q)] = \frac{\partial^2\hat{\phi}(\eta,q)}{\partial\eta^2} + Sc\left(\hat{f}(\eta,q)\frac{\partial\hat{\phi}(\eta,q)}{\partial\eta} - \frac{\partial\hat{f}(\eta,q)}{\partial\eta}\hat{\phi}(\eta,q)\right)$$
$$-Sc\tau\left(\frac{\partial\hat{\theta}(\eta,q)}{\partial\eta}\frac{\partial\hat{\phi}(\eta,q)}{\partial\eta} - \hat{\phi}(\eta,q)\frac{\partial^2\hat{\theta}(\eta,q)}{\partial\eta^2}\right). \qquad (28)$$

When $q = 0$ and $q = 1$, one has

$$\hat{f}(\eta;0) = f_0(\eta); \hat{f}(\eta;1) = f(\eta), \tag{29}$$

$$\hat{\theta}(\eta;0) = \theta_0(\eta); \hat{\theta}(\eta;1) = \theta(\eta), \tag{30}$$

$$\hat{\phi}(\eta;0) = \phi_0(\eta); \hat{\phi}(\eta;1) = \phi(\eta). \tag{31}$$

Note that, when q increases from 0 to 1, then $f(\eta,q)$, $\theta(\eta,q)$ and $\phi(\eta,q)$ approach $f_0(\eta)$ to $f(\eta)$, $\theta_0(\eta)$ to $\theta(\eta)$ and $\phi_0(\eta)$ to $\phi(\eta)$. According-ing to Taylor's series, one has:

$$f(\eta,q) = f_0(\eta) + \sum_{m=1}^{\infty} f_m(\eta)q^m,$$
$$f_m(\eta) = \frac{1}{m!} \left. \frac{\partial^m f(\eta;q)}{\partial \eta^m} \right|_{q=0}, \tag{32}$$

$$\theta(\eta,q) = \theta_0(\eta) + \sum_{m=1}^{\infty} \theta_m(\eta)q^m,$$
$$\theta_m(\eta) = \frac{1}{m!} \left. \frac{\partial^m \theta(\eta;q)}{\partial \eta^m} \right|_{q=0}, \tag{33}$$

$$\phi(\eta,q) = \phi_0(\eta) + \sum_{m=1}^{\infty} \phi_m(\eta)q^m,$$
$$\phi_m(\eta) = \frac{1}{m!} \left. \frac{\partial^m \phi(\eta;q)}{\partial \eta^m} \right|_{q=0}. \tag{34}$$

The convergence of series (22)-(24) is closely associated with $\hbar_f$, $\hbar_\theta$ and $\hbar_\phi$. The values of $\hbar_f$, $\hbar_\theta$ and $\hbar_\phi$ are chosen such that the series (22)-(24) converge at $q = 1$. Thus

$$f(\eta) = f_0(\eta) + \sum_{m=1}^{\infty} f_m(\eta), \tag{35}$$

$$\theta(\eta) = \theta_0(\eta) + \sum_{m=1}^{\infty} \theta_m(\eta), \tag{36}$$

$$\phi(\eta) = \phi_0(\eta) + \sum_{m=1}^{\infty} \phi_m(\eta). \tag{37}$$

The general solutions for f_m, θ_m and ϕ_m in terms of special solutions f_m^*, θ_m^* and ϕ_m^* are

$$f_m(\eta) = f_m^*(\eta) + C_1 + C_2 e^\eta + C_3 e^{-\eta}, \tag{38}$$

$$\theta_m(\eta) = \theta_m^*(\eta) + C_4 e^\eta + C_5 e^{-\eta}, \tag{39}$$

$$\phi_m(\eta) = \phi_m^*(\eta) + C_6 e^\eta + C_7 e^{-\eta}. \tag{40}$$

CONVERGENCE ANALYSIS AND DISCUSSION

The auxiliary parameters $\hbar_f$, $\hbar_\theta$ and $\hbar_\phi$ play an important role in controlling and adjusting the convergence of the series solutions. To find a suitable value for each of these auxiliary parameters, the $\hbar -$ curves at the $19th$ order of approximation are displayed. Figure 2 indicates that the admissible values of $\hbar_f$, $\hbar_\theta$ and $\hbar_\phi$ are $-1.10 \le \hbar_f \le -0.20$, $-1.20 \le \hbar_\theta \le -0.10$ and $-1.20 \le \hbar_\phi \le -0.20$. Our series solutions converge in the whole region of η for $\hbar_f = \hbar_\theta = \hbar_\phi = -0.7$.
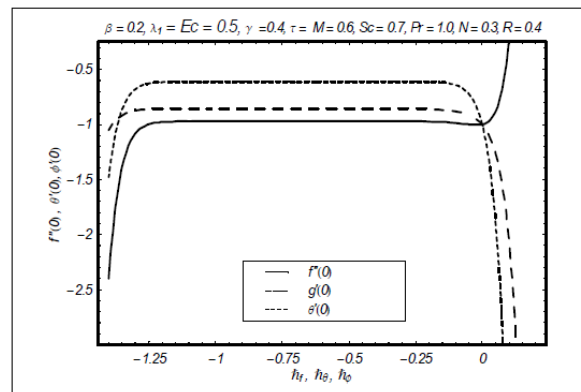

Figure 2: $\hbar -$ curves for the functions f, θ and ϕ

Figures 3-18 plot the effects of the various interesting parameters on the velocity $f'(\eta)$, temperature $\theta(\eta)$ and concentration $\phi(\eta)$. The fluid velocity and momentum boundary layer thickness increase with an increase in Deborah number β (see Figure 3). In Figure 4, the influence of the ratio of relaxation to the retardation times is sketched for the fluid velocity. It shows that the fluid velocity decreases upon increasing λ_1. Figure 5 shows that an increase in the

local buoyancy parameter γ yields an increase in the velocity. In fact, the local buoyancy parameter depends on the buoyancy force and an increase in buoyancy force gives rise to the fluid velocity increase. An increase in Hartmann number M decreases the fluid velocity (see Figure 6). The Hartmann number is a consequence of the Lorentz force. Obviously an increase in the Lorentz force opposes the flow and thus the fluid velocity decreases. Figure 7 shows that

the velocity and momentum boundary layer thickness are decreasing functions of the Prandtl number Pr. Figure 8 displays the effects of the ratio of buoyancy parameter N. The effects of the ratio of the buoyancy parameter are similar to that of γ in a qualitative way. The difference we noticed is that the fluid velocity increases more rapidly in the case of increasing local buoyancy parameter when compared with the ratio of the buoyancy parameter.
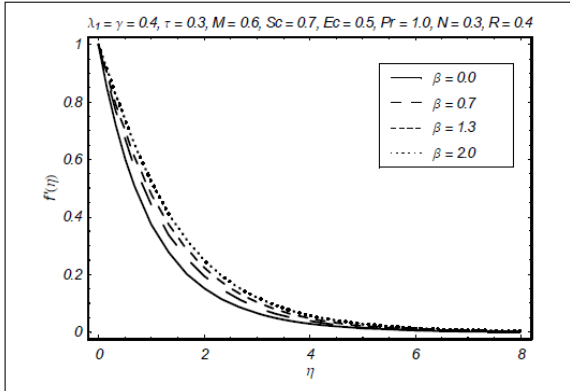

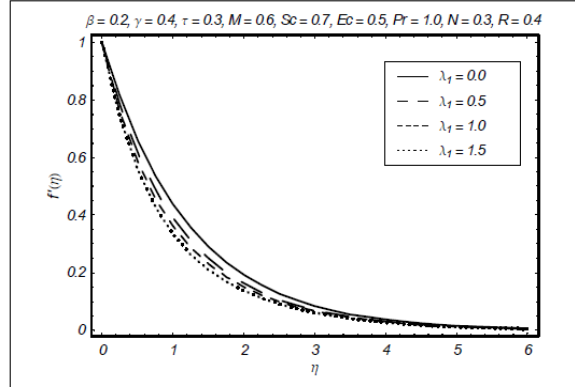**Figure 3:** Effect of β on velocity $f'(\eta)$

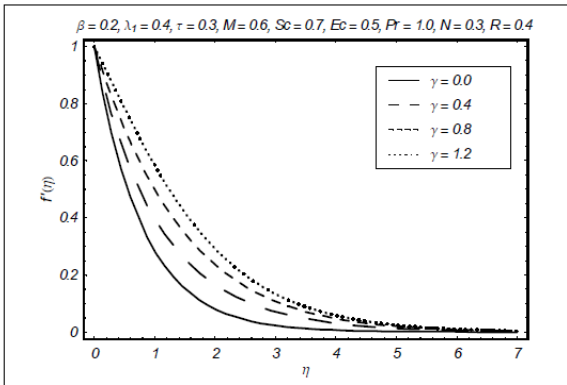**Figure 4:** Effect of λ_1 on velocity $f'(\eta)$

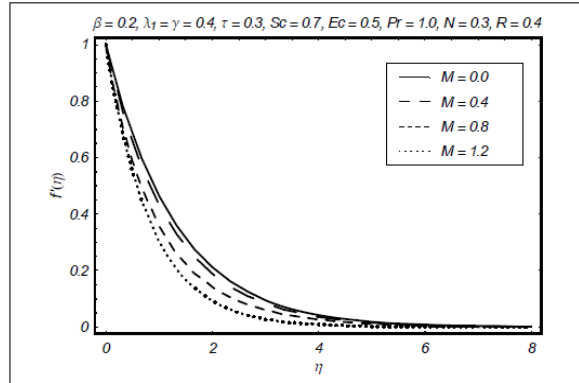**Figure 5:** Effect of γ on velocity $f'(\eta)$

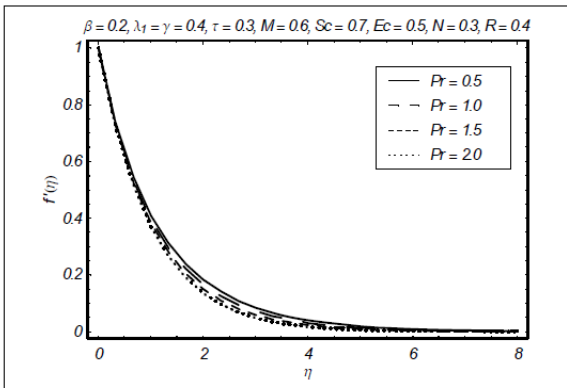**Figure 6:** Effect of M on velocity $f'(\eta)$

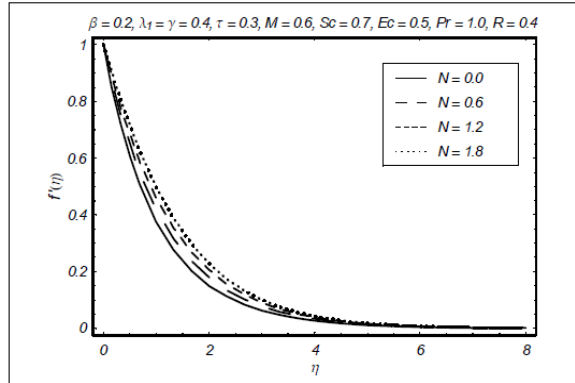**Figure 7:** Effect of Pr on velocity $f'(\eta)$

Figure 8: Effect of N on velocity $f'(\eta)$

Effects of different parameters on the temperature are seen in Figures 9-14. Figure 9 depicts the effects of the local buoyancy parameter on the temperature field. The temperature field and thermal boundary layer thickness are reduced with an increase in γ. Figure 10 shows that the temperature increases when the Hartmann number is increased. In fact, large M corresponds to lower permeability and hence the temperature and the thermal boundary layer thickness increase. Figures 11 and 12 illustrate the influences of Eckert number Ec and Prandtl number Pr on the temperature. It is observed from these figures that Ec and Pr have quite opposite effects on the velocity and the associated thermal boundary layer thickness. The temperature profile decreases more quickly for Ec in comparison to Pr. The ratio of the buoyancy parameter and the radiation parameter correspond to a decrease and an increase in the temperature, respectively (see Figures 13 and 14).
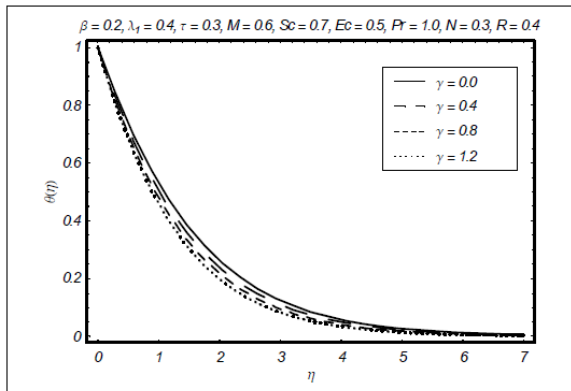

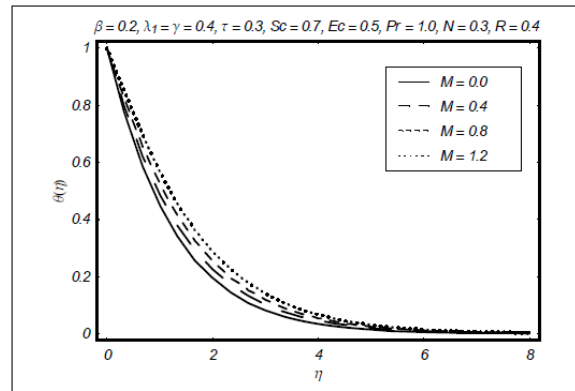**Figure 9:** Effect of γ on temperature $\theta(\eta)$

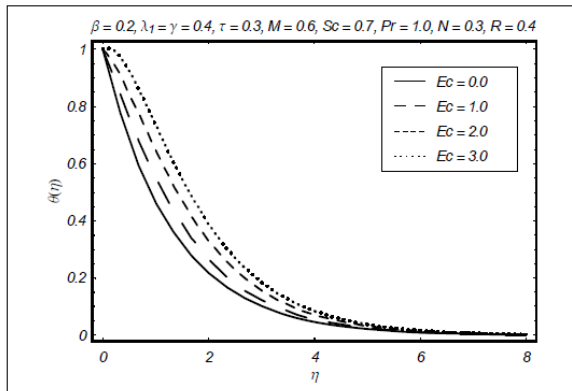**Figure 10:** Effect of M on temperature $\theta(\eta)$

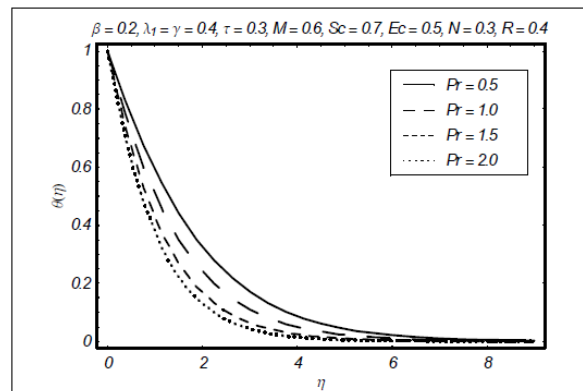**Figure 11:** Effect of Ec on temperature $\theta(\eta)$

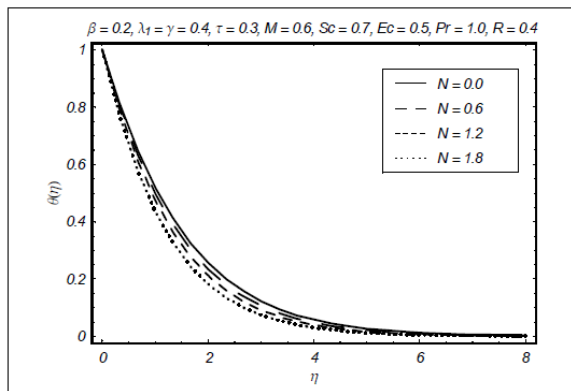**Figure 12:** Effect of Pr on temperature $\theta(\eta)$

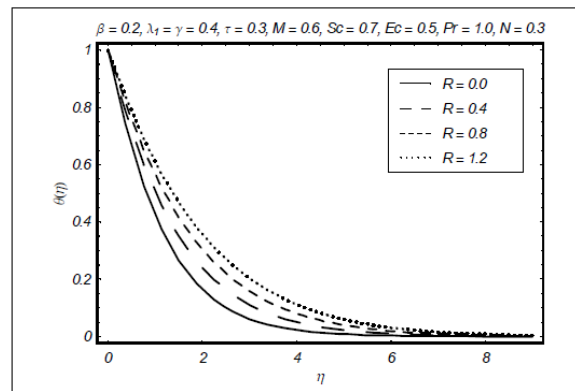**Figure 13:** Effect of N on temperature $\theta(\eta)$

Figure 14: Effect of R on temperature $\theta(\eta)$

The effects of γ, M, N and R on concentration profile are seen through Figures 15-18. Figure 15 shows that the concentration and boundary layer thickness are decreasing functions of γ. It is found from Figure 16 that the Hartmann number increases the concentration profile and associated boundary layer thickness. The effects of N and R on $\phi(\eta)$ are similar. Increases in N and R decrease the concentration and related boundary layer thickness (see Figures 17 and 18). It is worth mentioning here that the effects of M on the temperature are more pronounced when compared with the concentration. This same observation also holds for the influences of γ, N and R on the temperature and concentration.

Table 1 shows the convergence of the series solutions through computations of numerical values. This table indicates that our series solutions converge from the 20th-order of deformations for velocity and temperature and 25th-order of approximation for the concentration. Table 2 includes the numerical values of the skin-friction coefficient for the different values of β, λ_1, τ, M, Sc Sc, Ec and Pr when $N = 0.3$ and $R = 0.4$. The skin-friction coefficient increases with increasing β, M, Sc and Pr. It decreases when λ_1, γ and Ec are increased. Interestingly the variation in the values of the skin-friction coefficient is very small with increasing thermophoretic parameter τ. Table 3 consists of the values of the local Nusselt and Sherwood numbers. The values of the local Nusselt and Sherwood numbers increase slowly in comparison to the increase in the values of the skin-friction coefficient when β increases. The increase in the values of the local Nusselt number is very small upon increasing τ, but the increase in the values of the local Sherwood number is large. A comparative study of Tables 2 and 3 shows that the values of the skin-friction coefficient and local Sherwood number are larger than the values of the local Nusselt number.

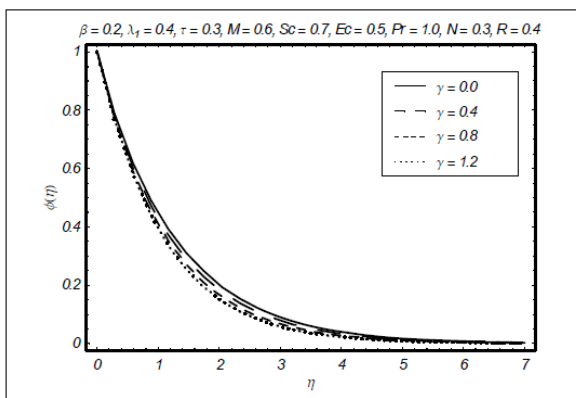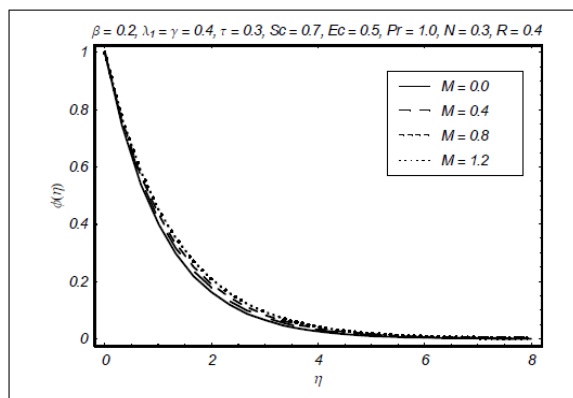**Figure 15:** Effect of γ on concentration $\phi(\eta)$

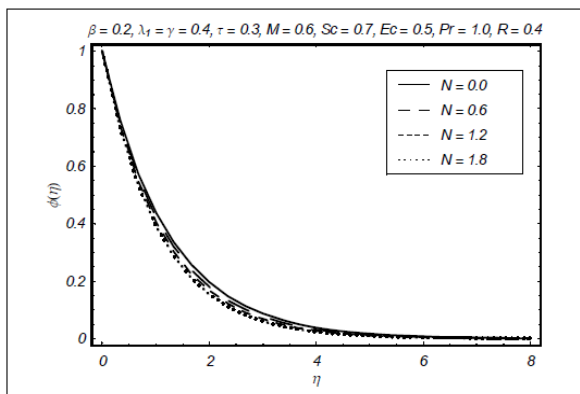**Figure 16:** Effect of M on concentration $\phi(\eta)$

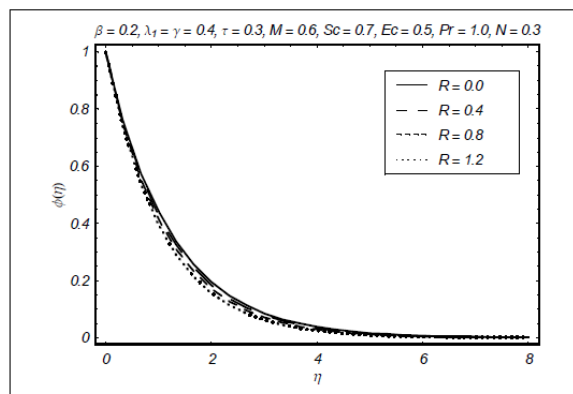**Figure 17:** Effect of N on concentration $\phi(\eta)$

Figure 18: Effect of R on concentration $\phi(\eta)$

Table 1: Convergence of series solutions for different order of approximations when $\beta = 0.2$, $\gamma = 0.4$, $\tau = M = 0.6$, $Sc = 0.7$, $\lambda = Ec = 0.5$, $Pr = 1.0$, $N = 0.3$, $R = 0.4$ and $\hbar_f = \hbar_\theta = \hbar_\phi = -0.7$.

Order of approximations	$-f''(0)$	$-\theta'(0)$	$-\phi(0)$
1	1.03150	0.66750	0.89500
5	0.99364	0.61878	0.85224
10	0.99306	0.61970	0.84720
20	0.99305	0.61974	0.84646
25	0.99305	0.61974	0.84643
30	0.99305	0.61974	0.84643
35	0.99305	0.61974	0.84643

Table 2: Numerical values of skin-friction coefficient for different values of β, λ_1, τ, , M, Sc, Ec and Pr when $N = 0.3$ and $R = 0.4$.

β	λ_1	γ	τ	M	Sc	Ec	Pr	$\frac{1}{1+\lambda_1}(f''(0)+\beta f'''(0))$
0.0	0.5	0.3	0.6	0.5	0.7	0.5	1.0	0.71413
0.5								0.90356
0.8								1.0027
0.3	0.0							1.0491
	0.4							0.86561
	0.7							0.77473
		0.0						1.0408
		0.5						0.70657
		1.0						0.41345
			0.0					0.83167
			1.0					0.83249
			2.0					0.83348
				0.0				0.71759
				0.7				0.93320
				1.0				1.1251
					0.5			0.82715
					1.0			0.83743
					1.5			0.84318
						0.4		0.83355
						0.7		0.82934
						1.0		0.82517
							0.8	0.82329
							1.4	0.84533
							2.0	0.85857

Table 3: Numerical values of local Nusselt number $-\theta'(0)$ and local Sherwood number $-\phi'(0)$ for different values of β, λ_1, τ, M, Sc, Ec and Pr when N=0.3 and R=0.4.

β	λ_1	γ	τ	M	Sc	Ec	Pr	$-\theta'(0)$	$-\phi'(0)$
0.0	0.5	0.3	0.6	0.5	0.7	0.5	1.0	0.59817	0.83428
0.5								0.64563	0.86222
0.8								0.66635	0.87576
0.3	0.0							0.67517	0.88177
	0.4							0.63701	0.85682
	0.7							0.61469	0.84353
		0.0						0.51553	0.77548
		0.5						0.67418	0.88124
		1.0						0.74023	0.93082
			0.0					0.62941	0.81539
			1.0					0.62886	0.87961
			2.0					0.62821	0.96235
				0.0				0.70545	0.86946
				0.7				0.56261	0.83748
				1.0				0.43885	0.81203
					0.5			0.63443	0.66407
					1.0			0.62439	1.1064
					1.5			0.62040	1.4825
						0.4		0.65805	0.84409
						0.7		0.57159	0.86747
						1.0		0.48634	0.88986
							0.8	0.55885	0.86466
							1.4	0.74998	0.82693
							2.0	0.8992	0.79074

CLOSING REMARKS

In this study we discussed the effects of thermal radiation, Joule heating and thermophoresis in stretched flow of a Jeffrey fluid. The main observations are as follows:

- Effects of β and λ_1 on the fluid velocity are quite opposite.
- An increase in the ratio of the buoyancy parameter N corresponds to an increase in $f'(\eta)$.
- The fluid temperature rises with an increase in Eckert number Ec.
- Effects of the ratio of the buoyancy parameter and radiation parameter are qualitatively similar.
- Variations in temperature are more pronounced than those in concentration when M increases.
- The increase in the values of the skin-friction coefficient and the local Nusselt number is very small in comparison to the increase in the local Sherwood number when τ increases.
- Numerical values of the local Nusselt number increase and the values of the local Sherwood number decrease with increasing Prandtl number Pr.

REFERENCES

Aslam, M. S., Rahman, M. M. and Sattar, M. A., Effects of variable suction and thermophoresis on

steady MHD combined free-forced convective heat and mass transfer flow over a semi-infinite permeable inclined plate in the presence of thermal radiation. Int. J. Thermal Sci., 47, p. 758 (2008).

Aziz, R. C., Hashim, I. and Abbasbandy, S., Effects of thermocapillarity and thermal radiation on flow and heat transfer in a thin liquid film on an unsteady stretching sheet. Math. Problems Eng., DOI:10.1155/2012/127320.

Bhattacharyya, K., Mukhopadhyay, S. and Layek, G. C., Slip effects on an unsteady boundary layer stagnation-point flow and heat transfer towards a stretching sheet. Chin. Phy. Lett., 28, p. 09470 (2001).

Goren, S. L., Thermophoresis of aerosol particles in laminar boundary layer on flat plate. J. Colloid Interf. Sci., 61, p. 77 (1977).

Haitao, Q. and Mingyu, X., Unsteady flow of viscoelastic fluid with fractional Maxwell model in a channel. Mech. Research Commun., 34, p. 210 (2007).

Hayat, T. and Alsaedi, A., On thermal radiation and Joule heating effects in MHD flow of an Oldroyd-B fluid with thermophoresis. Arab. J. Sci. Eng., 36, p. 1113 (2011).

Hayat, T. and Qasim, M., Influence of thermal radiation and Joule heating on MHD flow of a Maxwell fluid in the presence of thermophoresis. Int. J. Heat Mass Transfer, 53, p. 4780 (2010).

Hayat, T., Qasim, M. and Abbas, Z., Radiation and mass transfer effects on the magnetohydrodynamic unsteady flow induced by a stretching sheet. Z Naturforsch A. 64, p. 231 (2010).

Hayat, T., Shehzad, S. A. and Qasim, M., Mixed convection flow of a micropolar fluid with radiation and chemical reaction. Int. J. Num. Methods Fluids, 67, p. 1418 (2011).

Hayat, T., Shehzad, S. A., Qasim, M. and Obaidat, S., Flow of a second grade fluid with convective boundary conditions. Thermal Sci., 15, p. S253 (2011).

Hayat, T., Shehzad, S. A., Qasim, M. and Obaidat, S., Radiative flow of Jeffery fluid in a porous medium with power law heat flux and heat source. Nuclear Eng. Design, 243, p. 15 (2012).

Hayat, T., Shehzad, S. A., Qasim, M. and Obaidat, S., Steady flow of Maxwell fluid with convective boundary conditions. Z. Naturforsch 66a, p. 417 (2011).

Hayat, T., Shehzad, S. A., Qasim, M. and Obaidat, S., Thermal radiation effects on the mixed convection stagnation-point flow in a Jeffery fluid. Z. Naturforsch 66a, p. 606 (2011).

Hinds, W. C., Aerosol Technology: Properties, Behavior, and Measurement of Airborne Particles. John Wiley and Sons, New York, (1982).

Jamil, M. and Fetecau, C., Helical flows of Maxwell fluid between coaxial cylinders with given shear stresses on the boundary. Nonlinear Analysis: Real World Appl., 11, p. 4302 (2010).

Jamil, M. and Fetecau, C., Some exact solutions for rotating flows of a generalized Burgers' fluid in cylindrical domains. J. Non-Newtonian Fluid Mech., 165, p. 1700 (2010).

Jamil, M., Khan, N. A. and Zafar, A. A., Translational flows of an Oldroyd-B fluid with fractional derivatives. Comput. Math. Appl., 62, p. 1540 (2011).

Kothandapani, M. and Srinivas, S., Peristaltic transport of a Jeffrey fluid under the effect of magnetic field in an asymmetric channel. Int. J. Non-Linear Mech 43, p. 915 (2008).

Liao, S. J., Beyond Perturbation: Introduction to Homotopy Analysis Method. Chapman and Hall, CRC Press, Boca Raton (2003).

Makinde, O. D. and Aziz, A., Boundary layer flow of a nano fluid past a stretching sheet with convective boundary conditions. Int. J. Thermal. Sci., 50, p. 1326 (2011).

Nadeem, S. and Akbar, N. S., Peristaltic flow of a Jeffrey fluid with variable viscosity in an asymmetric channel. Zeitschrift fur Naturforschung A 64, p. 713 (2010).

Nadeem, S., Zaheer, S. and Fang, T., Effects of thermal radiation on the boundary layer flow of a Jeffery fluid over an exponentially stretching surface. Numer. Algor., 57, p. 187 (2011).

Noor, N. F. M., Abbasbandy, S. and Hashim, I., Heat and mass transfer of thermophoretic MHD flow over an inclined radiate isothermal permeable surface in the presence of heat source/sink. Int. J. Heat Mass Transfer, 55, 2122 (2012).

Rashidi, M. M. and Erfani, E., A new analytical study of MHD stagnation-point flow in porous media with heat transfer. Comput. Fluids, 40, p. 172 (2011).

Rashidi, M. M. and Pour, S. A. M., Analytic approximate solutions for unsteady boundary-layer flow and heat transfer due to a stretching sheet by homotopy analysis method. Nonlinear Analysis: Modelling and Control, 15, p. 83 (2010).

Rashidi, M. M., Pour, S. A. M. and Abbasbandy, S., Analytic approximate solutions for heat transfer of a micropolar fluid through a porous medium with radiation. Commun. Nonlinear Sci. Numer. Simulat., 16, p. 1874 (2011).

Rashidi, M. M., Pour, S. A. M. and Abbasbandy, S.,

Analytic approximate solutions for heat transfer of a micropolar fluid through a porous medium with radiation. Commun. Nonlinear Sci. Numer. Simulat., 16, p. 1874 (2011).

Sahoo, B. and Poncet, S., Flow and heat transfer of a third grade fluid past an exponentially stretching sheet with partial slip boundary condition. Int. J. Heat Mass Transfer, 54, p. 5010 (2011).

Tasai, C. J., Lin, J. S., Shankar, I., Aggarwal, G. and Chen, D. R., Thermophoretic deposition of particles in laminar and turbulent tube flows. Aerosol Sci. Tech., 38, p. 131 (2004).

Vosughi, H., Shivanian, E. and Abbasbandy, S., A new analytical technique to solve Volterra's integral equations. Math. Methods Appl. Sci. 34, p. 1243 (2011).

Vyas, P. and Rai, A., Radiative flow with variable thermal conductivity over a non-isothermal stretching sheet in a porous medium. Int. J. Contemp. Math. Sciences, 5, p. 2685 (2010).

Wang, S. and Tan, W. C., Stability analysis of soret-driven double-diffusive convection of Maxwell fluid in a porous medium. Int. J. Heat Fluid Flow 32, p. 88 (2011).

Yao, B., Approximate analytical solution to the Falkner-Skan wedge flow with the permeable wall of uniform suction, Commun. Nonlinear Sci. Numer. Simulat. 14, p. 3320 (2009).

Yao, S., Fang, T. and Zhang, J., Heat transfer of a generalized stretching/shrinking wall problem with convective boundary conditions. Comm. Nonlinear Sci. Num. Simu. 16, p. 752 (2011).